International Journal of Remote Sensing
Vol. 29, No. 6, 20 March 2008, 1825–1832

Letter

Emissivity errors in the vegetation cover method caused by the lack of atmospheric correction

L. MARTINEZ*†, V. CASELLES‡, V. PALA† and E. VALOR‡

†Institut Cartogràfic de Catalunya, Parc de Montjuïc s/n, E-08038 Barcelona, Spain
‡Departament de Física de la Terra i Termodinàmica, Universitat de València, Dr. Moliner 50, E-46100 Burjassot, Spain

(*Received 14 February 2007; in final form 24 November 2007*)

The influence of the lack of atmospheric correction of the optical images used to calculate land surface emissivity (LSE) was assessed. When thermal emissivity is determined by the vegetation cover method (VCM), information from the solar spectrum is required to calculate the vegetation cover fraction. The atmospheric correction was obtained in this study by using a combination of the dark dense vegetation (DDV) method and the Second Simulation of the Satellite Signal in the Solar Spectrum (6S) code. The methodology was applied to a Landsat Thematic Mapper (TM) image of Tomelloso, Spain. We determined that the emissivity between 10 and 12 μm only increases by 0.4% (which represents a systematic error of approximately +0.2 K) when atmospherically corrected reflectances are used in relation to non-corrected Tomelloso scenes. Nevertheless, other test areas could yield larger differences.

1. Introduction

Land surface temperature (LST) estimation by means of passive thermal remote sensing depends on accurate emissivity specification (Becker 1987). Land surface emissivity (LSE) measurement by remote sensing has the disadvantage that the temperature and emissivity cannot be calculated simultaneously because the number of unknown variables is always higher than the number of measurements. To overcome this, qualitative approximations are used, for example assuming a constant value of the emissivity for all bands or introducing a hypothesis such as relating emissivity to some of the vegetation variables. The vegetation cover method (VCM) developed by Valor and Caselles (1996) is based on the relationship between emissivity in the thermal infrared and the normalized difference vegetation index (NDVI) suggested by Van de Griend and Owe (1993). As a consequence, it is expected that the determination of thermal emissivity is affected to a certain extent by the interaction of the atmosphere with the solar radiation, which is the subject of this letter.

The atmospheric effect is sometimes not significant (Song *et al*. 2001), but this is not the general case. There are many procedures described in the literature for obtaining a reflectance free of atmospheric effects on multispectral satellite sensors. The most accurate are those based on both simultaneous in-field measurements of the atmospheric variables, such as aerosol optical thickness (AOT) in the study area,

*Corresponding author. Email: lucas.martinez@icc.cat

International Journal of Remote Sensing
ISSN 0143-1161 print/ISSN 1366-5901 online
http://www.tandf.co.uk/journals
DOI: 10.1080/01431160701824632

and the use of a radiative transfer code (Bolle and Langer 1991). To do that, one of the most popular codes is the Second Simulation of the Satellite Signal in the Solar Spectrum (6S), described by Vermote *et al*. (1997). Nevertheless, intermediate and more operational solutions may also be adopted, such as the use of an atmospheric normalization method (Holben 1986, Caselles and López 1989) or the use of standard values for the atmospheric variables (Pons and Solé-Sugrañes 1994).

As mentioned, there are several atmospheric variables (such as the AOT) to be calculated or measured to apply a radiation transfer code. As a simultaneous AOT measurement is not usually available, there are several methods to determine it by means of remote sensing imagery. Many works reference the dark dense vegetation (DDV) approximation of Liang *et al*. (1997) and the contrast reduction (CD) of Tanré *et al*. (1998). The former is easy to apply, whereas the later was designed for a multitemporal case and therefore requires several images.

The aim of this study was to measure the influence of the atmospheric correction on the estimate of thermal emissivity with the VCM. A combination of the 6S and DDV methods was used, which proved to be operational and accurate, with no need to use data collected in field campaigns or multitemporal series.

2. Methodology

2.1 *The VCM*

The VCM is a model for the LSE of a pixel that provides the effective emissivity of a heterogeneous and rough surface, ε, as:

$$\varepsilon = \varepsilon_v P_V + \varepsilon_g (1 - P_V) + 4\langle d\varepsilon \rangle P_V (1 - P_V) \tag{1}$$

where ε_v represents vegetation emissivity, P_V is the fractional vegetation cover, ε_g is bare soil emissivity and $<d\varepsilon>$ is the cavity term that is related to the radiance emitted indirectly through internal reflections occurring between crop walls and the ground (Valor and Caselles 1996). Emissivity values for vegetation and bare soil can be measured in the field (Rubio *et al.* 1996) or obtained from a database (Salisbury and D'Aria 1992).

Determination of the fractional vegetation cover is calculated using the NDVI, with the following expression (Valor and Caselles 1996):

$$P_V = \frac{\left(1 - \frac{NDVI}{NDVI_G}\right)}{\left(1 - \frac{NDVI}{NDVI_G}\right) - K\left(1 - \frac{NDVI}{NDVI_V}\right)} \tag{2}$$

where $NDVI_G$ and $NDVI_V$ represent the minimal and maximum values of the NDVI image, respectively, which, provided that the area is large enough, will correspond with areas with no vegetation (bare soil) and with full vegetation coverage.

The K parameter for a Landsat TM set of bands is calculated as (Valor and Caselles 1996):

$$K = \frac{\rho_{4V} - \rho_{3V}}{\rho_{4G} - \rho_{3G}} \tag{3}$$

where ρ_{4V} and ρ_{3V} are the reflectances in the near-infrared (TM band 4) and in the red (TM band 3) for the area with full vegetation cover, and ρ_{4G} and ρ_{3G} the reflectances in the near-infrared and in the red for the area without vegetation (bare

soil). Valor and Caselles (1996) reported that the VCM error varies between 0.5% and 2.0%, depending on whether the values used for ε_g and ε_v are measured as field or global standard estimates.

2.2 *The DDV and 6S methods*

The absorption effect of the atmospheric gases and the dispersion effect of gases and aerosols are simulated by means of the 6S code. The system needs several input variables to characterize the atmosphere. The accuracy of the simulations of 6S depends on the quality of the atmospheric variables (Vermote *et al.* 1997).

The DDV method is based on the use of dark areas with dense vegetation, and the signal received by the sensor comes to a great extent from the atmosphere (Kaufman and Sendra 1988). According to Ouaidrari and Vermote (1999), at the bottom of the atmosphere (BOA) for the DDV areas and using Landsat TM images, the reflectance in the blue ($\rho^1{}_b$) can be calculated from the middle infrared reflectance ($\rho^7{}_b$) using the following equation:

$$\rho_b^1 = \frac{\rho_b^7}{4.3} \tag{4}$$

In the same way, the reflectance in the red ($\rho^3{}_b$) can be calculated using the following expression:

$$\rho_b^3 = \frac{\rho_b^7}{2.0} \tag{5}$$

The DDV method for the measurement of the AOT is shown graphically in figure 1. The following paragraphs describe the relationships between top of the atmosphere (TOA) and BOA reflectances with the aim of determining the AOT.

First, the DDV areas are selected, at the TOA image, using a simple reflectance threshold in the middle infrared (TM band 7). Then, a mean value of the reflectance in the middle infrared ($\rho^7{}_t$) is calculated. The TOA reflectance value ($\rho^7{}_t$) is corrected atmospherically with the 6S method using the clean atmosphere hypothesis (with no aerosol) to obtain an estimate of the DDV reflectance at the BOA for the middle infrared ($\rho^7{}_{b'}$). With the reflectance at the BOA for the middle infrared ($\rho^7{}_{b'}$) it becomes possible to estimate the DDV reflectance at the BOA for the blue and red channels, ($\rho^1{}_{b'}$) and ($\rho^3{}_{b'}$), using equations (4) and (5).

Then, using the estimate of reflectance at the BOA for the blue and red channels, ($\rho^1{}_{b'}$) and ($\rho^3{}_{b'}$), it is possible to simulate blue and red TOA reflectances ($\rho^1{}_{t'}$ and $\rho^3{}_{t'}$) for a series of aerosol AOT values at $\lambda = 550$ nm by means of the 6S code. Next, the reflectances at the TOA for the DDV areas and the corresponding AOTs at $\lambda = 550$ nm are tabulated for each channel (blue and red). In the tables calculated previously, the reflectances of the DDV in the blue ($\rho^1{}_t$) and red ($\rho^3{}_t$) at the TOA and other AOT values are interpolated. τ_1 represents the AOT at $\lambda = 550$ nm obtained with the blue channel, and τ_3 that of the red one. Finally, as τ_1 and τ_3 are two estimates of the same parameter (AOT at $\lambda = 550$ nm), they are expected to be identical.

Once the AOT at $\lambda = 550$ nm is calculated by means of the DDV method, the next step is to perform the atmospheric correction of the imagery. This is done with the 6S method, using the AOT value obtained before.

Kaufman *et al.* (1997) reported that the accuracy of the DDV method for the measurement of the AOT was estimated as $\pm 0.06\,\mathrm{m}^{-1}$. The absolute error of the

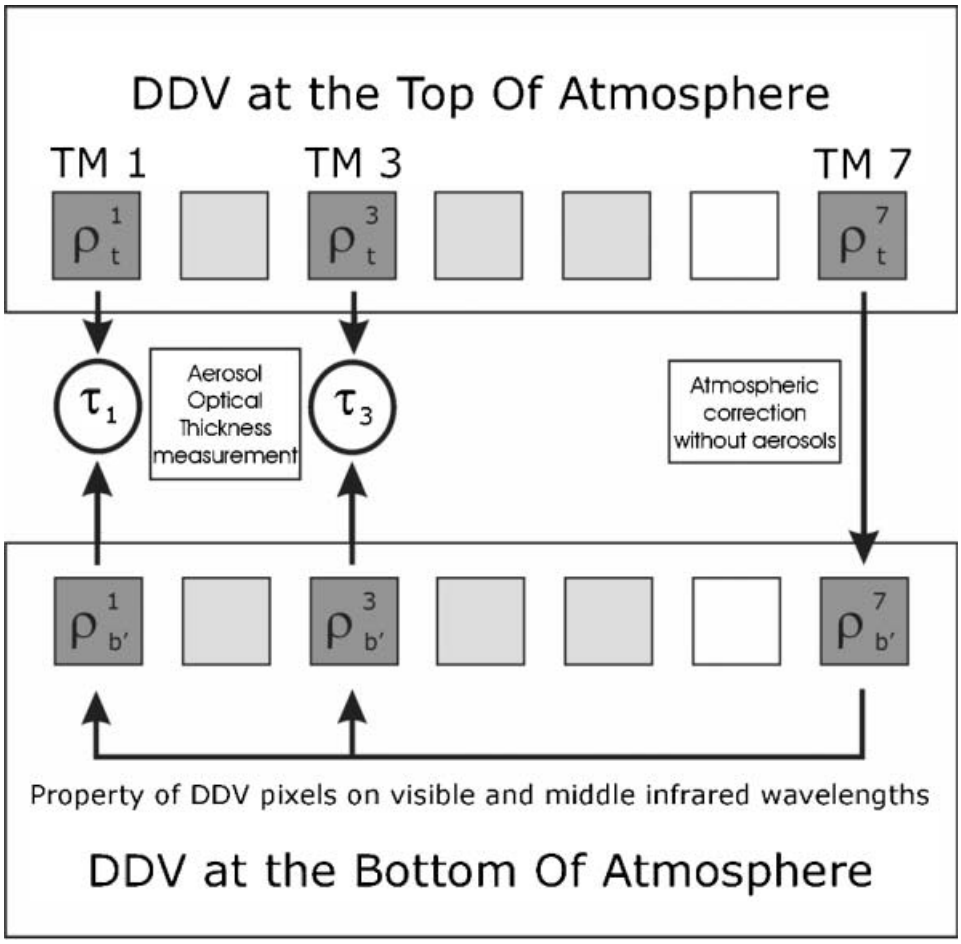

Figure 1. Procedure for the measurement of aerosol optical thickness (AOT) using the 6S and DDV methods. DDVs TOA middle infrared reflectance is atmospherically corrected without aerosols and provides an estimation of the BOA blue and red reflectances. These BOA reflectances are compared with the actual TOA blue and red reflectances by using a radiative transfer code to yield an estimation of the AOT at 550 nm.

reflectance calculated using the aforementioned combination of 6S and DDV was estimated as ± 0.015 for the visible channels and ± 0.08 in the near infrared, according to Ouaidrari and Vermote (1999).

3. Results

The methodology described was applied to a scene in the Tomelloso area, which is located in the northeastern end of the province of Ciudad Real (Spain), in what can be considered the centre of the natural region of La Mancha. It is a fairly uniform area, at approximately 670 m above sea level, without significant differences in height. The landscape is arid, with little woodland and vineyard plantations. The climate is Mediterranean with continental features; the middle temperature ranges from 5°C in the coldest month to 26°C in the warmest, with a mean annual precipitation of 350 mm (Artigao *et al.* 2005). In the Tomelloso area in Ciudad Real,

for the interval 10–12 μm, field measurements by Artigao *et al.* (2005) yielded $\varepsilon_g=0.975$ and $\varepsilon_v=0.987$, and the cavity term was estimated as $<d\varepsilon>=0.011$ from field measurements of the vegetation geometry.

The atmospheric correction method proposed was applied to a Landsat 5 TM image subscene (1124 × 1124 pixels) taken on 23 August 1994 at 10:05 GMT and centred at geographical coordinates 2.9195 W and 39.1256 N (WGS84 geodetic data), as shown in figure 2. This image is simultaneous to the field data acquisition of Artigao *et al.* (2005). First, the DDV areas in the image were selected using an adequate reflectance threshold for DDVs of 0.1 in the middle infrared TOA reflectance. The mean reflectances and the standard deviations for the whole set of selected DDV areas at the TOA were $\rho^7{}_t=0.088\pm0.006$ (TM 7, middle infrared), $\rho^1{}_t=0.122\pm0.004$ (TM 1, blue) and $\rho^3{}_t=0.082\pm0.005$ (TM 3, red).

The reflectance for the middle infrared was corrected atmospherically using the 6S code considering an atmosphere with no aerosol, and it was found that at the BOA, $\rho^7{}_{b'}=0.100\pm0.006$ (TM 7, middle infrared). Next, by means of equations (4) and (5) we determined that at the BOA, $\rho^1{}_{b'}=0.0233\pm0.0014$ (TM 1, blue) and $\rho^3{}_{b'}=0.050\pm0.003$ (TM 3, red).

Then the AOT was obtained. For this purpose, table 1 was elaborated by using the 6S code. By linear interpolation of the table the result was $\tau_1=0.369\pm0.011$ and $\tau_3=0.37\pm0.02$. The small difference between both values shows that the aerosol and atmosphere models selected were suitable.

Afterwards, the red and near-infrared channels were atmospherically corrected with the 6S code. For this purpose, a table search procedure and subsequent linear interpolation for each image pixel was implemented.

To analyse the effect of the atmospheric correction on the thermal emissivity values, the subscenes A and B of figure 2 were used. They do not include urbanized areas or road links, and the existing water has been blacked out for convenience. Based on the NDVI histogram, first a pixel was identified as pure soil and another

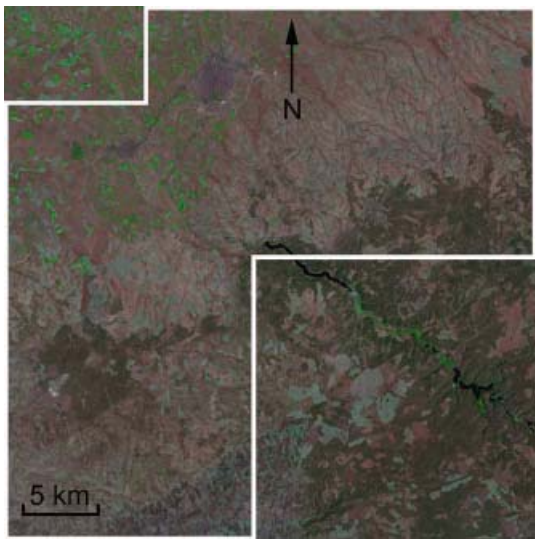

Figure 2. Tomelloso test area in Ciudad Real (Spain). Image centre coordinates 39.1256 N and 2.9195 W (WGS84 geodetic data). Landsat TM RGB image of the area on 23 August 1994 at 10:05 GMT (subscene A: upper left corner; subscene B: lower right corner).

Table 1. Estimate of the aerosol optical thickness (AOT) at 550 nm by DDV methodology.

AOT at 550 nm (m^{-1})	TOA blue reflectance $\rho^1{}_t$	TOA red reflectance $\rho^3{}_t$
0.4389	0.1276	0.0854
0.4067	0.1248	0.0838
0.3794	0.1225	0.0826
0.3559	0.1206	0.0815
0.3354	0.1189	0.0806
0.3174	0.1175	0.0798

one as pure vegetation; this was done for the subscenes of the reflectance images at the TOA and at the BOA. With these bare land and vegetation pixels, the reflectance in the red and near-infrared was measured, as well as the corresponding NDVIs. Then the proportion of vegetation and thermal emissivity was calculated using equations (2) and (1), respectively. Table 2 shows the results obtained.

Table 3 shows the variation of several quantities with and without the atmospheric correction of the VCM method: although the reflectances in the red and near-infrared, the vegetation index and fractional vegetation cover vary substantially, the thermal emissivity only increases by 0.4%. Nevertheless, according to Becker (1987), this increase causes a systematic error of approximately $+0.2$ K in the temperature value.

The uncertainty of the vegetation cover does not cause a large systematic error in the emissivity and the corresponding temperature value. This is because the vegetation and ground emissivities for the area studied are close. A doubling of the increase obtained would result in 0.8% in terms of emissivity and a systematic error of approximately $+0.4$ K in the temperature value (Becker 1987). Those differences could be generated by using the same uncertainty of the vegetation cover and vegetation emissivity but with a smaller value for the ground emissivity. On this hypothesis the required ground emissivity value would be $\varepsilon'_g = 0.935 \pm 0.005$. This emissivity value is realistic for these grounds and illustrates that other test areas could generate larger differences.

4. Conclusions

In this letter the 6S and DDV methods are combined to implement an operational atmospheric correction procedure for the effects of the emissivity calculations. The method has been applied to a Landsat TM subscene in the Tomelloso area (Ciudad

Table 2. Mean values for the subscenes A and B of the red and near-infrared reflectance, NDVI, fractional vegetation cover and thermal emissivity at the top (TOA) and bottom of the atmosphere (BOA). Despite the large variability in fractional vegetation cover, it has a minimum impact on 10–12 μm emissivity for the test area.

	Red reflectance (TM 3)	Near-infrared reflectance (TM 4)	NDVI	Fractional vegetation cover (P_v)	Thermal emissivity
Subscene A					
TOA	0.21 ± 0.05	0.44 ± 0.07	0.35 ± 0.11	0.15 ± 0.16	0.978 ± 0.006
BOA	0.23 ± 0.06	0.52 ± 0.08	0.39 ± 0.12	0.24 ± 0.19	0.981 ± 0.005
Subscene B					
TOA	0.17 ± 0.05	0.33 ± 0.08	0.33 ± 0.05	0.20 ± 0.07	0.981 ± 0.003
BOA	0.18 ± 0.07	0.39 ± 0.09	0.39 ± 0.08	0.31 ± 0.11	0.985 ± 0.004

Table 3. Variation in reflectance, NDVI, P_v, emissivity and temperature when using atmospherically corrected reflectances in the emissivity estimate with the VCM.

	Increase
Red reflectance (TM 3) (%)	8
Near-infrared reflectance (TM 4) (%)	18
NDVI (%)	15
P_v (%)	58
Emissivity (%)	0.4
Temperature (K)	0.2

Real, Spain). The vegetation index and proportion showed a substantial increase when using atmospherically corrected reflectances but only a 0.4% increase was detected in the emissivity. Nonetheless, this increase causes a systematic error in the temperature measurement of approximately +0.2 K. Finally, it is concluded that other test areas could yield larger differences in the emissivity when using atmospherically corrected reflectances.

Acknowledgements

We thank Drs Eva María Rubio and María del Mar Artiago of Castilla La Mancha University for the information provided on the Tomelloso image, and Dr Eric F. Vermote of Maryland University for his explanations concerning the atmospheric correction.

References

ARTIGAO, M.M., RUBIO, E.M. and CASELLES, V., 2005, Actual evapotranspiration in a vineyard of Spain. In *Recent Research Developments in Thermal Remote Sensing*, V. Caselles, E. Valor and C. Coll (Eds), pp. 135–155 (Kerala: Research Signpost).

BECKER, F., 1987, The impact of spectral emissivity on the measurement of land surface temperatures from a satellite. *International Journal of Remote Sensing*, **8**, pp. 1509–1522.

BOLLE, H.J. and LANGER, I., 1991, *Echival Field Experiment in a Desertification-threatened Area (EFEDA)* (Germany: Meteorological Institute, Free University of Berlin).

CASELLES, V. and LÓPEZ, M.J., 1989, An alternative simple approach to estimate atmospheric correction in multitemporal studies. *International Journal of Remote Sensing*, **10**, pp. 1127–1134.

HOLBEN, B.N., 1986, Characteristics of maximum-value composite images from temporal AVHRR data. *International Journal of Remote Sensing*, **7**, pp. 1417–1434.

KAUFMAN, Y.J. and SENDRA, C., 1988, Algorithm for automatic corrections to visible and near-infrared satellite imagery. *International Journal of Remote Sensing*, **9**, pp. 1357–1381.

KAUFMAN, Y.J., WALD, A.E., REMER, L.A., GAO, B.C., LI, R.R. and FLYNN, L., 1997, The MODIS 2.1 μm channel – correlation with visible reflectance for use in remote sensing of aerosol. *IEEE Transactions on Geoscience and Remote Sensing*, **35**, pp. 675–686.

LIANG, S., FALLAH-ADL, H., KALLURI, S., JAJA, J., KAUFMAN, Y. and TOWNSHEND, J., 1997, An operational atmospheric correction algorithm for Landsat Thematic Mapper imagery over land. *Journal of Geophysical Research*, **102**, pp. 173–186.

OUAIDRARI, H. and VERMOTE, E., 1999, Operational atmospheric correction of Landsat TM data. *Remote Sensing of Environment*, **70**, pp. 4–15.

PONS, X. and SOLÉ-SUGRAÑES, L., 1994, A simple radiometric correction model to improve automatic mapping of vegetation from multispectral satellite data. *Remote Sensing of Environment*, **48**, pp. 191–204.

RUBIO, E., CASELLES, V. and BADENAS, C., 1997, Emissivity measurements of several soils and vegetation types in the 8-14 μm waveband: analysis of two field methods. *Remote Sensing of Environment*, **59**, pp. 490–521.

SALISBURY, J.W. and D'ARIA, D.M., 1992, Emissivity of terrestrial materials in the 8-14 μm atmospheric window. *Remote Sensing of Environment*, **42**, pp. 83–106.

SONG, C., WOODCOCK, C.E., SETO, K.C., LENNEY, M.P. and MACOMBER, S.A., 2001, Classification and change detection using Landsat TM data: when and how to correct atmospheric effects? *Remote Sensing of Environment*, **75**, pp. 230–244.

TANRÉ, D., DESCHAMPS, P.Y., DEVAUX, C. and HERMAN, M., 1988, Estimation of Saharan aerosol optical thickness from blurring effects in Thematic Mapper data. *Journal of Geophysical Research*, **93**, pp. 15955–15964.

VALOR, E. and CASELLES, V., 1996, Mapping land surface emissivity from NDVI: applications to European, African, and South American areas. *Remote Sensing of Environment*, **57**, pp. 167–184.

VAN DE GRIEND, A.A. and OWE, M., 1993, On the relationship between thermal emissivity and the normalized difference vegetation index for natural surfaces. *International Journal of Remote Sensing*, **14**, pp. 1119–1131.

VERMOTE, E., TANRÉ, D., DEUZÉ, J.L., HERMAN, M. and MORCRETTE, J.J., 1997, Second simulation of the satellite signal in the solar spectrum, 6S: an overview. *IEEE Transactions on Geoscience and Remote Sensing*, **35**, pp. 675–686.